Electronic Supplementary Information

Balancing the phosphorescence and fluorescence of a double-ring porphyrin using different lanthanides for ratiometric oxygen sensing

Huimin Zhao[a, †, *], Qingqing Wang[a, †], Shumin Wang[a], Junyue Yin[a], Huibin Wang[a], Wenhao Shao[b], Zixin Yao[a], Jianting Yao[c], Lixin Zang[a, *]

[a]*College of Chemistry, Chemical Engineering and Materials Science, Shandong Provincial Engineering and Technical Center of Light Manipulations, Shandong Provincial Key Laboratory of Optics and Photonic Device, School of Physics and Electronics, Shandong Normal University, Ji'nan 250014, China*

[b]*Davidson School of Chemical Engineering, Purdue University, West Lafayette, IN 47907, USA*

[c]*Department of Ultrasound in Medicine and Research Center of Ultrasound in Medicine and Biomedical Engineering, the 2nd Affiliated Hospital of Zhejiang University School of Medicine, Zhejiang University, Hangzhou 310009, China*

Corresponding Authors: hmzhao_hit@hotmail.com,+86-13066026354 (H.Z.); lxzang@sdnu.edu.cn, +86-18946006021 (L.Z.).

[†]*These authors contributed equally.*

I. Preparation and purification of the samples

Gadolinium(III)-coordinated sinoporphyrin sodium (Gd$_2$-DVDMS) was synthesized as follows. Briefly, a mixture of imidazole (6 g), DVDMS (12 mg, ~10 μmol), and excess anhydrous GdCl$_3$ (53 mg, ~200 μmol) was added to a 250 mL three-necked bottle under a flow of argon over a period of 30 min. The mixture was then heated to and maintained at 200 °C, and stirred magnetically, for 2 h under a flow of argon. After cooling to room temperature, the mixture was dissolved in methanol to yield 10 mL of Gd$_2$-DVDMS solution. For praseodymium-coordinated DVDMS (Pr$_2$-DVDMS) and neodymium-coordinated DVDMS (Nd$_2$-DVDMS), the synthesis procedures were almost the same as that of Gd$_2$-DVDMS, with PrCl$_3$·6H$_2$O (71 mg, ~200 μmol) and NdCl$_3$ (51 mg, ~200 μmol), respectively, used instead of the GdCl$_3$. For the mixed-lanthanide(III) DVDMS complexes, taking praseodymium and gadolinium-coordinated DVDMS (PrGd-DVDMS) as an example, the synthesis procedure was almost identical to that for Gd$_2$-DVDMS, with excess anhydrous GdCl$_3$ (26 mg, ~100 μmol) and PrCl$_3$·6H$_2$O (36 mg, ~100 μmol) being used together in place of the GdCl$_3$. The as-prepared metalloporphyrin solution was purified by dialysis (dialysis membrane, molecular weight cut off = 1000). It was dialyzed three times using methanol as the solvent, with each dialysis step lasting 2 h. During this process, low molecular weight species, such as imidazole, lanthanide ions, and anions, were eliminated from the metalloporphyrin solution.

II. Determination of photoluminescence lifetimes

A square wave was given to a diode laser controller (Thorlabs ITC510) to control a diode laser centered at 405 nm (Thorlabs TCLDM9). Phosphorescence signals were recorded by a grating spectrometer (Zolix Omni-λ300) and amplified by a photomultiplier tube (Zolix PMTH-S1-R212) with a high-voltage power supply (Zolix HVC1800). The time-resolved signal was averaged with a digital phosphor oscilloscope (Tektronix DPO5054) and the decay curve was sent to a personal computer to determine its lifetime. The phosphorescence lifetime evaluation was performed by fitting the decay curve to an exponential function using adjustable parameters.

To determine the fluorescence lifetime, a 1-MHz pulsed laser centered at 392 nm was used as the light source. Fluorescence signals were recorded as a function of time using a spectrofluorometer (HORIBA, Fluoromax-4). The fluorescence lifetime evaluation was performed by fitting the decay curve (fluorescence intensity) to an exponential function using adjustable parameters.

III. Determination of luminescence quantum yields

The luminescence quantum yield (Φ) of the studied metalloporphyrins in air-saturated methanol solution was measured using a comparative method. Gadolinium-labeled hematoporphyrin monomethyl ether (Gd-HMME) was used as the reference ($\Phi = 0.014$ in methanol).[1] The relationship between the Φ_P of the studied metalloporphyrin and that of Gd-HMME can be expressed as follows:[2]

$$\Phi_P = \Phi_r (\frac{I}{A})(\frac{A_r}{I_r}), \tag{S1}$$

where Φ_r and Φ_P are the phosphorescence quantum yields of Gd-HMME and the

studied metalloporphyrin, respectively, in methanol. I_r and I are the integrated emission intensities of Gd-HMME and the studied metalloporphyrin, respectively, under 532-nm laser illumination. A is the absorption of the methanolic metalloporphyrin solution at 532 nm, calculated from Equation (S2) from measurements obtained using a power meter (Ophir 199728):

$$A = (I_{\text{methanol}} - I_{\text{metalloporhyrin}})/I_{\text{methanol}}, \tag{S2}$$

where I_{methanol} is the power per unit area of the light transmitted by the blank solvent (methanol), and $I_{\text{metalloporhyrin}}$ is the power per unit area of the light transmitted by the methanolic metalloporphyrin solution.

IV. The measurement of singlet oxygen generation efficiency

The singlet oxygen generation efficiencies of Pr_2-DVDMS, Gd_2-DVDMS, and PrGd-DVDMS were investigated using a 532-nm solid-state laser as the excitation source. The generation of singlet oxygen was measured by monitoring the consumption of the singlet oxygen scavenger DPBF at the central wavelength of its absorption band (410 nm). The singlet oxygen quantum yields (Φ_Δ) of Pr_2-DVDMS, Gd_2-DVDMS, and PrGd-DVDMS were evaluated using a relative method with Gd-HMME as the reference.[3] This relative method was based on Equation (S3):

$$\Phi_\Delta = \Phi_{\Delta,r}(\frac{k}{A})(\frac{A_r}{k_r}). \tag{S3}$$

In Equation (S3), the subscript "r" indicates the reference reagent, k is the degradation rate of the singlet oxygen scavenger, and A is the absorption of the excitation light by

the metalloporphyrin, which was calculated using Equation (S2) from measurements obtained using a power meter (Ophir 199728).

V. Characterization of Pr₂-DVDMS, Gd₂-DVDMS, and PrGd-DVDMS

Figure S1 shows the UV–visible absorption spectra of (a) DVDMS, (b) Pr$_2$-DVDMS, (c) Gd$_2$-DVDMS, and (d) PrGd-DVDMS. The reduction in the number of Q bands in the absorption spectra of the three studied metalloporphyrins from four to two confirmed that the metalloporphyrins was successfully synthesized.
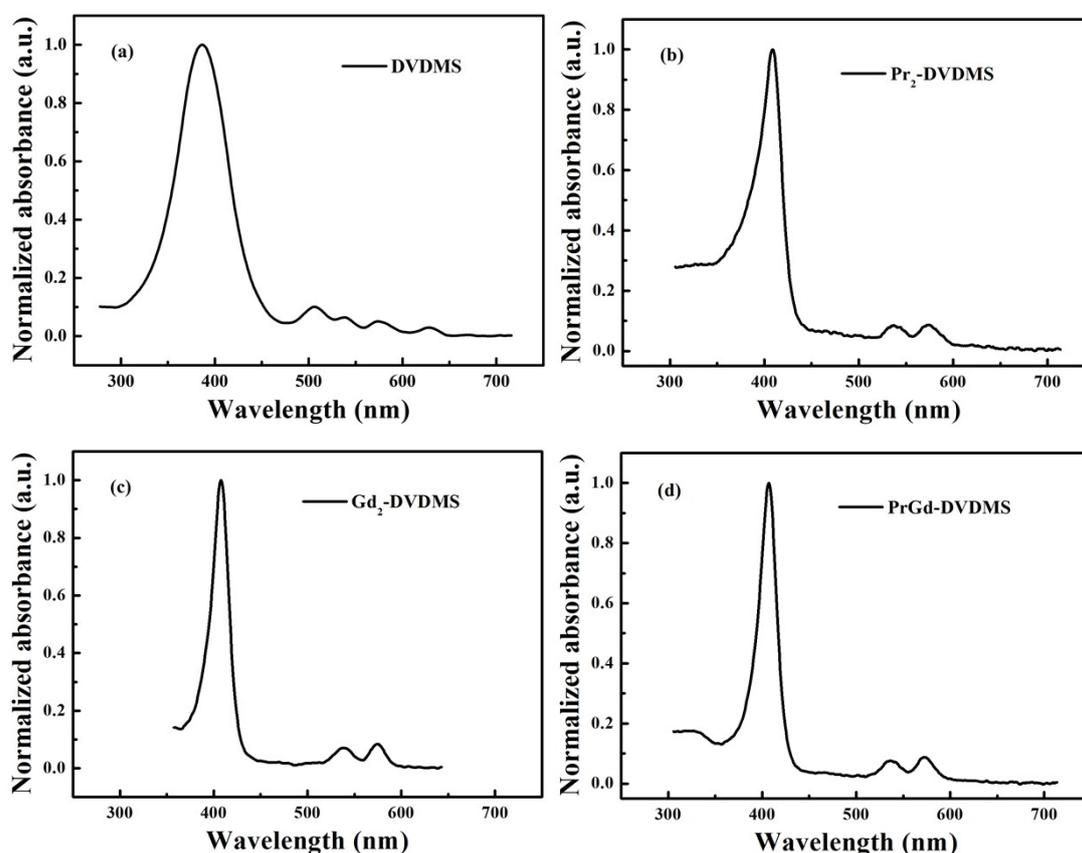
Figure S1. Normalized UV–visible absorption spectra of (a) DVDMS, (b) Pr$_2$-DVDMS, (c) Gd$_2$-DVDMS, and (d) PrGd-DVDMS.

The mass spectra of DVDMS and the studied metalloporphyrins were recorded on a MALDI-TOF mass spectrometer (RapifleX MALDI-TOF/TOF MS, Bruker Daltonics, Germany). Figure S2 shows (a) the experimental mass spectrum and (b) the

theoretical mass spectrum of DVDMS ([DVDMS+5H−4Na]$^+$,C$_{68}$H$_{71}$N$_8$O$_9$$^+$), (c) the

experimental mass spectrum and (b) the theoretical mass spectrum of Gd$_2$-DVDMS

([DVDMS+2Gd−4H−4Na]$^+$, C$_{68}$H$_{62}$N$_8$O$_9$Gd$_2$$^+$). The *m/z* peak of DVDMS appeared at

1143.526, the shape of which corresponds well to [DVDMS+5H−4Na]$^+$ (C$_{68}$H$_{71}$O$_9$$^+$,

1143.534) and is in good agreement with the reported results for DVDMS.[4] The *m/z*

peak of Gd$_2$-DVDMS appeared at 1450.217, the shape of which corresponds well to

[DVDMS+2Gd−4H−4Na]$^+$ (C$_{68}$H$_{62}$O$_9$Gd$_2$$^+$, 1450.314).
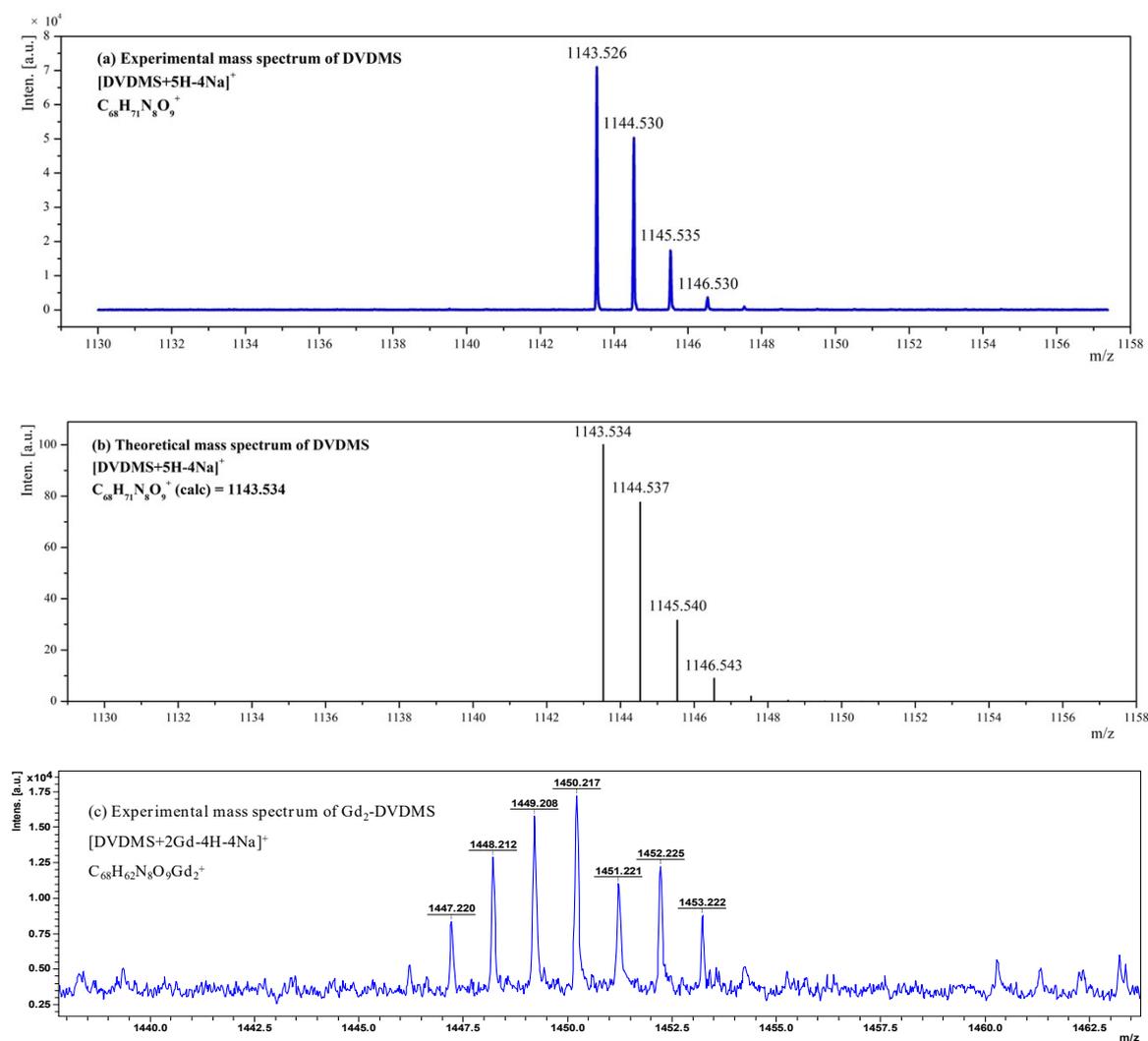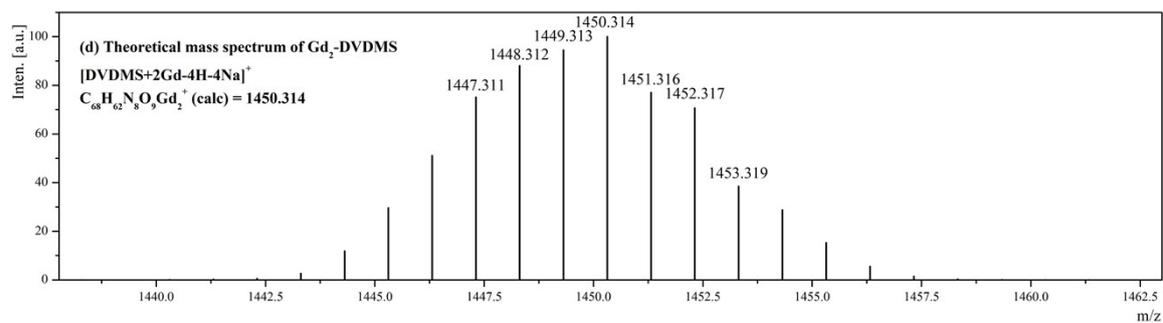
Figure S2. (a) The experimental mass spectrum (positive mode) and (b) theoretical mass spectrum of DVDMS ([DVDMS+5H−4Na]$^+$,$C_{68}H_{71}N_8O_9^+$), (c) the experimental mass spectrum (positive mode) and (d) theoretical mass spectrum of Gd$_2$-DVDMS ([DVDMS+2Gd−4H−4Na]$^+$, $C_{68}H_{62}N_8O_9Gd_2^+$).

VI. Metalloporphyrin chemical structures
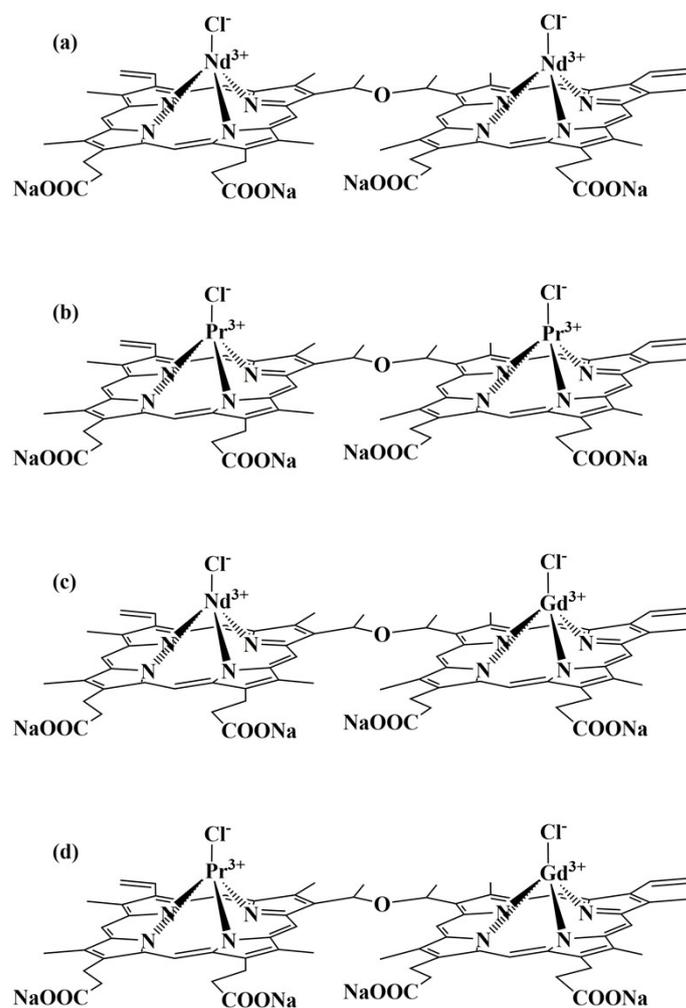
Figure S3. Chemical structures of (a) Nd$_2$-DVDMS, (b) Pr$_2$-DVDMS, (c) NdGd-DVDMS, and (d) PrGd-DVDMS.

VII. The fluorescence lifetime of Pr$_2$-DVDMS and PrGd-DVDMS

The fluorescence decay curves of Pr$_2$-DVDMS and PrGd-DVDMS at 626 nm are shown in Figure S4.
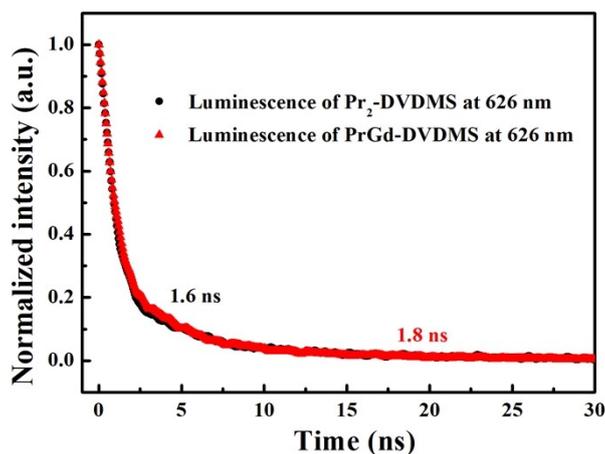
Figure S4. Fluorescence decay curves of Pr$_2$-DVDMS and PrGd-DVDMS measured at λ_{em} = 626 nm.

VIII. Computational study of state-switching mechanism

The computation for the simplest porphyrin, porphine, and its metalloporphyrins (Pr-porphine and Gd-porphine) was performed, the chemical structures of which are shown in Figure S5a. Geometry optimization and vertical excitation energy calculations were carried out by means of density functional theory (DFT) and time-dependent density functional theory (TD-DFT) calculations, implemented in the Gaussian 16 package using the PBE0 functional[5] in vacuum. 6-31g(d,p) basis set was used for light elements (C, N, H) while the Stuttgart effective core potentials[6] were used for Gd (MWB54) and Pr (MWB49). Spin–orbit coupling (SOC) was calculated in the Dalton 2020 package[7] using the same functional and basis set combination in

vacuum based on the ground-state geometry optimized in Gaussian 16. Input geometry and molecular orbitals for Dalton were generated using the molecular orbital KIT (MOKIT) package to accurately account for the basis set choice for fast convergence. Natural transition orbitals (NTOs) were visualized using the multiwfn package.[8]

As seen from Figure S5, the SOC matrix element (SOCME) for T_1-S_0 transition increased from 0.161 for porphine free-base, to 0.316 for Pr-porphine, and to 0.414 for Gd-porphine. The larger SOC for Gd-porphine indicates the higher radiative constant for the triplet to ground state emission. Furthermore, the lowest excited energy level of Gd(III) is higher than both the S_1 and T_1 states of porphyrins, and hence nonradiative relaxation from a porphyrin to Gd(III) cannot occur.[3] Thus, both the higher SOC and special energy level of Gd(III) result in the state switching and triplet phosphorescence emission. The enhanced SOC efficiencies originate from the orbital contribution of heavy Gd and Pr to the T_1-S_0 transition of porphyrin, as pointed out by the red arrows in Figure S5.

It is worth to point out that current basis sets used for Gd (MWB54) and Pr (MWB49) consider their 4f electrons as pseudopotentials (as well as the entire inner core $1s^2 2s^2 2p^6 3s^2 3p^6 3d^{10} 4s^2 4p^6 4d^{10} 4f^x$), and thus the degree of their electronic contribution to the molecular orbitals of porphyrin is weak, leading to low enhancement in SOC efficiency. Theoretically if explicated consider the 4f electrons in heavy metals and only treat a smaller core ($1s^2 2s^2 2p^6 3s^2 3p^6 3d^{10}$) as pseudopotential, such as using MWB28 or def2-QZVP as basis set, larger contribution from metal

electrons could be anticipated, as well as much larger SOCMEs. Although our current computation methods have not been advanced to complete the full calculation from geometry optimization to SOCMEs, we have included the NTOs of T_1-S_0 transition for Pr-porphyrin complex calculated with MWB28 basis set for Pr (Figure S5b). Indeed, adequate contribution of Pr atomic orbitals was observed in the T_1-S_0 transition of porphyrin.
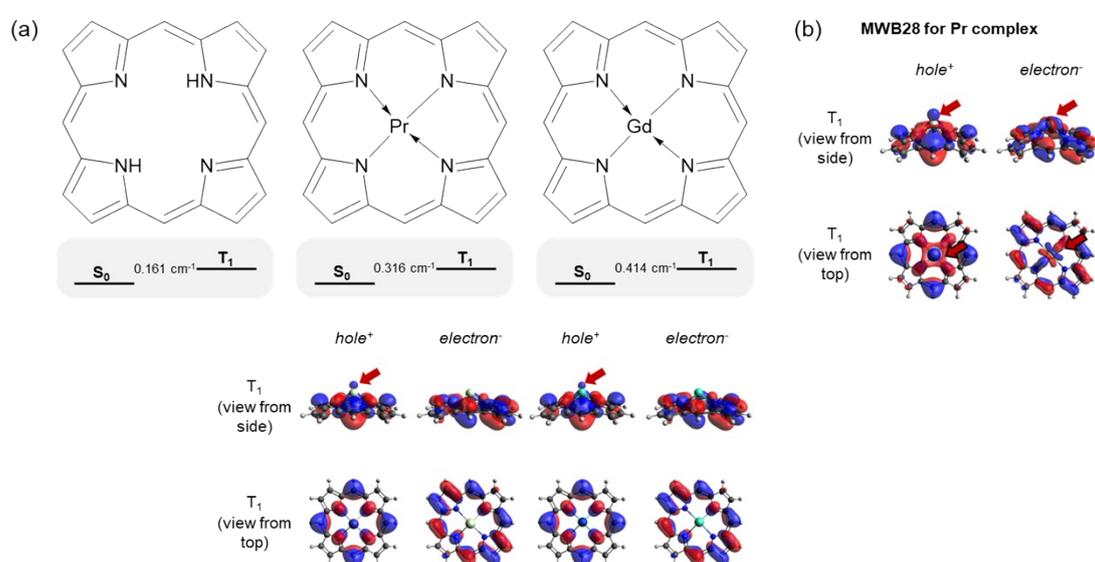
Figure S5. Computation results for porphine, Pr-porphine and Gd-porphine. (a) molecular structure of porphine and its Gd, Pr complexes; SOCMEs and NTOs of their T_1-S_0 transitions. Red arrows in NTOs mark the contribution from Gd and Pr electrons. (b) T_1-S_0 NTOs of Pr-porphine complex calculated using MWB28 for Pr. Since 4f electrons are explicated considered, larger contribution from Pr elections was observed.

IX. Phosphorescence-to-fluorescence ratio measurement uncertainties
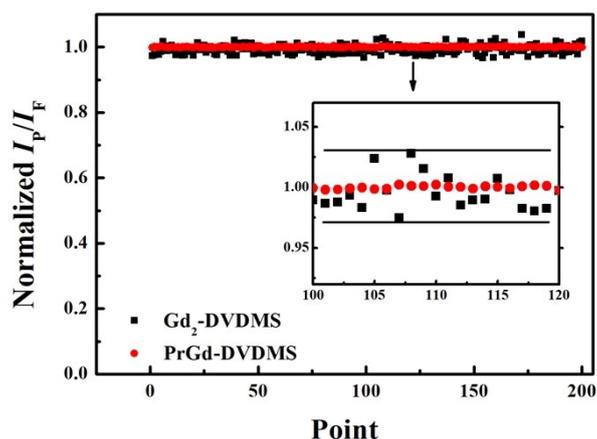
Figure S6. Normalized phosphorescence-to-fluorescence intensity ratios of PrGd-DVDMS and Gd₂-DVDMS showing the measurement uncertainties (the luminescence intensities were measured at the band maxima).

REFERENCES

1.   H. Zhao, L. Zang, H. Zhao, Y. Zhang, Y. Zheng, Z. Zhang and W. Cao, Oxygen sensing properties of gadolinium labeled hematoporphyrin monomethyl ether based on filter paper. *Sensors Actuators B: Chem.*, 2015, **206**, 351-356.

2.   F. Su, R. Alam, Q. Mei, Y. Tian, C. Youngbull, R. H. Johnson and D. R. Meldrum, Nanostructured oxygen sensor--using micelles to incorporate a hydrophobic platinum porphyrin. *PLoS One*, 2012, **7**(3), e33390.

3.   P. Wang, F. Qin, L. Wang, F. Li, Y. Zheng, Y. Song, Z. Zhang and W. Cao, Luminescence and photosensitivity of gadolinium labeled hematoporphyrin monomethyl ether. *Opt. Express*, 2014, **22**(3), 2414-2422.

4.   Q. Fang and D. Yang A dimer with two porphyrin salts bonded by ether and its preparation method. CN102030765A, 2011.

5.   C. Adamo and V. Barone, Toward reliable density functional methods without adjustable parameters: The pbe0 model. *J. Chem. Phys.*, 1999, **110**(13), 6158-6170.

6.   P. Schwerdtfeger, The pseudopotential approximation in electronic structure theory. *Chemphyschem*, 2011, **12**(17), 3143-3155.

7.   K. Aidas, C. Angeli, K. L. Bak, V. Bakken, R. Bast, L. Boman, O. Christiansen, R. Cimiraglia, S. Coriani, P. Dahle, E. K. Dalskov, U. Ekstrom, T. Enevoldsen, J. J. Eriksen, P. Ettenhuber, B. Fernandez, L. Ferrighi, H. Fliegl, L. Frediani, K. Hald, A. Halkier, C. Hattig, H. Heiberg, T. Helgaker, A. C. Hennum, H. Hettema, E. Hjertenaes, S. Host, I. M. Hoyvik, M. F. Iozzi, B. Jansik, H. J. Jensen, D. Jonsson, P. Jorgensen, J. Kauczor, S. Kirpekar, T. Kjaergaard, W. Klopper, S. Knecht, R. Kobayashi, H. Koch, J. Kongsted, A. Krapp, K. Kristensen, A. Ligabue, O. B. Lutnaes, J. I. Melo, K. V. Mikkelsen, R. H. Myhre, C. Neiss, C. B. Nielsen, P. Norman, J. Olsen, J. M. Olsen, A. Osted, M. J. Packer, F. Pawlowski, T. B. Pedersen, P. F. Provasi, S. Reine, Z. Rinkevicius, T. A. Ruden, K. Ruud, V. V. Rybkin, P. Salek, C. C. Samson, A. S. de Meras, T. Saue, S. P. Sauer, B. Schimmelpfennig, K. Sneskov, A. H. Steindal, K. O. Sylvester-Hvid, P. R. Taylor, A. M. Teale, E. I. Tellgren, D. P. Tew, A. J. Thorvaldsen, L. Thogersen, O. Vahtras, M. A. Watson, D. J. Wilson, M. Ziolkowski and H. Agren, The dalton quantum chemistry program system. *Wiley Interdiscip Rev Comput Mol Sci*, 2014, **4**(3), 269-284.

8.   T. Lu and F. Chen, Multiwfn: A multifunctional wavefunction analyzer. *J. Comput. Chem.*, 2012, **33**(5), 580-592.